1-1-2008

Raindrop size distribution measurements in tropical cyclones

Ali Tokay

Paul G. Bashor

Emad Habib

Takis Kasparis
University of Central Florida

Raindrop Size Distribution Measurements in Tropical Cyclones

ALI TOKAY

Joint Center for Earth Systems Technology, University of Maryland, Baltimore County, Baltimore, and NASA Goddard Space Flight Center, Greenbelt, Maryland

PAUL G. BASHOR

Computer Sciences Corporation, NASA Wallops Flight Facility, Wallops Island, Virginia

EMAD HABIB

Department of Civil Engineering, and Center for Louisiana Water Studies, University of Louisiana at Lafayette, Lafayette, Louisiana

TAKIS KASPARIS

School of Electrical Engineering and Computer Science, University of Central Florida, Orlando, Florida

(Manuscript received 14 December 2006, in final form 31 May 2007)

ABSTRACT

Characteristics of the raindrop size distribution in seven tropical cyclones have been studied through impact-type disdrometer measurements at three different sites during the 2004–06 Atlantic hurricane seasons. One of the cyclones has been observed at two different sites. High concentrations of small and/or midsize drops were observed in the presence or absence of large drops. Even in the presence of large drops, the maximum drop diameter rarely exceeded 4 mm. These characteristics of raindrop size distribution were observed in all stages of tropical cyclones, unless the storm was in the extratropical stage where the tropical cyclone and a midlatitude frontal system had merged. The presence of relatively high concentrations of large drops in extratropical cyclones resembled the size distribution in continental thunderstorms. The integral rain parameters of drop concentration, liquid water content, and rain rate at fixed reflectivity were therefore lower in extratropical cyclones than in tropical cyclones. In tropical cyclones, at a disdrometer-calculated reflectivity of 40 dBZ, the number concentration was 700 ± 100 drops m^{-3}, while the liquid water content and rain rate were 0.90 ± 0.05 g m^{-3} and 18.5 ± 0.5 mm h^{-1}, respectively. The mean mass diameter, on the other hand, was 1.67 ± 0.3 mm. The comparison of raindrop size distributions between Atlantic tropical cyclones and storms that occurred in the central tropical Pacific island of Roi-Namur revealed that the number density is slightly shifted toward smaller drops, resulting in higher-integral rain parameters and lower mean mass and maximum drop diameters at the latter site. Considering parameterization of the raindrop size distribution in tropical cyclones, characteristics of the normalized gamma distribution parameters were examined with respect to reflectivity. The mean mass diameter increased rapidly with reflectivity, while the normalized intercept parameter had an increasing trend with reflectivity. The shape parameter, on the other hand, decreased in a reflectivity range from 10 to 20 dBZ and remained steady at higher reflectivities. Considering the repeatability of the characteristics of the raindrop size distribution, a second impact disdrometer that was located 5.3 km away from the primary site in Wallops Island, Virginia, had similar size spectra in selected tropical cyclones.

1. Introduction

Flooding rainfall generated by tropical cyclones is generally attributed to the presence of abundant small and midsize drops. This conclusion is mainly driven through postanalysis of coincident radar and rain gauge observations where different forms of the radar reflectivity Z and rain rate R relations were applied to the radar measurement. The agreement between radar-estimated and gauge-measured rainfall is highly dependent on the coefficient and exponent of the Z–R relation (Vieux and Bedient 1998; Petersen et al. 1999). For

Corresponding author address: Ali Tokay, NASA Goddard Space Flight Center, Code 613.1, Greenbelt, MD 20771.
E-mail: tokay@radar.gsfc.nasa.gov

DOI: 10.1175/2007MWR2122.1

example, the National Weather Service's (NWS) Weather Surveillance Radar-1988 Doppler precipitation processing subsystem recommends $Z = 250R^{1.2}$ for tropical systems instead of the default $Z = 300R^{1.4}$, which is designed for continental convective systems (Fulton et al. 1998). Indeed, at reflectivities above 19 dBZ, the former Z–R relation results in higher rainfall than the latter one. This means that more small and midsize drops are present in the spectrum consistent with the former Z–R relation at a given reflectivity (>19 dBZ; Tokay et al. 2002). Although these studies hint at differences in the characteristics of the raindrop size distribution (RSD) between different systems, there is a wide range of uncertainty in the characteristics of the RSD, particularly in tropical cyclones.

There have been several studies of airborne RSD measurements in the eyewall and rainbands of hurricanes. Merceret (1974a) collected samples of raindrops with a foil impactor through aircraft penetrations in Hurricane Ginger (1971) and showed that the RSD is well represented by an exponential distribution. Foil impactors were also used to collect the samples of size spectra in Tropical Storm Felice (1970) and Hurricane Debby (1969). Scott (1974) who examined the datasets from these two storms reported exponential size distribution except the lack of small drops in the later storm. He attributed the lack of small drops to measurement errors. Merceret (1974b), who also examined the airborne spectra in Tropical Storm Felice, concluded the exponential distribution holds more above the cloud base than below the cloud base. The lack of small drops below the cloud base was evident and was attributed to the depletion of small drops.

Jorgensen and Willis (1982) derived Z–R relations based on data from four flights in three tropical cyclones. Unlike previous studies, the measurements were collected with an airborne optical probe. They reported no important differences in Z–R relations when the data were stratified by region (eyewall versus outside of eyewall), regime (convective versus stratiform), or altitude. Their best estimate was $Z = 300R^{1.35}$, which results in higher rainfall than NWS default Z–R, but much lower rainfall than NWS tropical Z–R at reflectivities above 25 dBZ. Willis (1984) and Willis and Tattelman (1989) used the same data but focused on the modeling aspects of the size spectra. Following Willis (1984), the size distribution from Hurricane Anita (1977) had abundant small drops and low concentrations of large drops even in very heavy rain. The size spectrum in very heavy rainfall was quite narrow, having maximum drop diameter around 4 mm.

Considering ground-based measurements, Wilson and Pollock (1974) reported $Z = 350R^{1.35}$ relation through Joss–Waldvogel (JW) disdrometer measurements taken during the passage of Hurricane Agnes (1972). At the time of observation, Hurricane Agnes was in tropical storm stage and the characteristics of RSD were not presented in this study. This particular Z–R relation yields less rainfall than the NWS default Z–R relation except above 44 dBZ, and it contradicts the airborne-based studies presented above. Ulbrich and Lee (2002), on the other hand, presented the characteristics differences in RSD prior to and during the passage of remnants of Hurricane Helene (2000) through JW disdrometer observations. They demonstrated drastically different Z–R relations prior to and during the passage of the remnants of Hurricane Helene, and also showed how the two operational Z–R relations mentioned above performed during different segments of the storm. Although the tropical Z–R performed better than the default relation, it still underestimated rainfall by 19%. The RSD had narrower spectra with higher number concentrations and lower median volume diameters during the passage of remnants of Hurricane Helene than in the prehurricane environment. Maeso et al. (2005) examined the characteristics of RSD through two-dimensional video disdrometer observations during the passage of Tropical Storm Jeanne (2004). The relatively low mean mass diameter and large value of the normalized intercept parameter (based on liquid water content) of the gamma function indicated that the air mass had oceanic characteristics.

The characteristics of RSD in tropical cyclones are also important for the representation of microphysical processes in mesoscale models. These models employ parameterized versions of the RSD based on aircraft probe measurements. McFarquhar and Black (2004), for example, presented the differences in parameters of the size distribution and mass-weighted fall speed drop diameter relations through aircraft measurements of Hurricane Norbert (1984) and Hurricane Emily (2004). In addition to the aircraft measurements, the parameters of the RSD can be retrieved from vertically pointed and polarimetric radar measurements (Williams 2002; Bringi et al. 2002) where the disdrometer-derived RSD parameters are employed to validate the retrieval algorithm.

This study presents disdrometer measurements of the RSD from seven tropical cyclones during the 2004–06 Atlantic hurricane seasons. In a number of cases, the remnants of the cyclone were at the tropical storm, tropical depression, and extratropical cyclone stage. The objective of this study is to determine the RSD characteristics between the different tropical cyclones particularly in the convective regime where rainfall is abundant. Prior to the discussion of the RSD in sections

5–7, the measurement sites and instruments are introduced in section 2 and the formulation of the RSD is presented in section 3. A brief synoptic setting is then provided to guide the reader through the history of the storms in section 4. We present the anatomy of the individual storms through a time series of the RSD in section 5 where the relative concentrations of small, midsize, and large drops are linked to the integral rain parameters. Unless otherwise noted, raindrops less than 1 mm in diameter are referred to as small drops, while the size ranges of 1 to 3 mm and larger than 3 mm represent the midsize and large drops, respectively. The comparison of the RSD between different storms is presented in section 6 where the composite spectra at 40 dBZ are constructed. It should be noted that this study does not use radar observations and the reflectivities mentioned here are strictly calculated from disdrometer measurements using the Raleigh approximation. We compare the characteristics of the RSD in tropical cyclones and in tropical oceanic systems in the central tropical Pacific Ocean in section 7. The parameters of the gamma model distribution at a given reflectivity in tropical cyclones and in the central tropical Pacific were presented in section 8. A summary and concluding remarks are given in section 9. The determination of the physical characteristics of the RSD from disdrometer measurement is not a straightforward task and measurement errors should be addressed. We address self-consistency of the disdrometer measurements through comparisons of the RSD observations from different units in the appendix.

2. Measurement sites and instruments

As part of the National Aeronautics and Space Administration (NASA) Tropical Rainfall Measuring Mission (TRMM) satellite validation program, a set of rain-measuring devices has been operating at Wallops Flight Facility, Wallops Island, Virginia, since 2000 (Tokay et al. 2005). Among the instruments, several impact-type JW disdrometers have been collecting samples of raindrop spectra nearly continuously over six years. In this study, we had six events where two or more JW disdrometers were operated during tropical cyclones. We have also used two tropical cyclone events—one in Lafayette, Louisiana, and the other in Orlando, Florida—where a JW disdrometer was operated. All three locations are also equipped with two or more tipping-bucket gauges collocated with the JW disdrometer.

The JW disdrometer (Joss and Waldvogel 1967) has been widely used in measuring RSD during the last four decades. It bins the measured drops between 0.3 and 5.3 mm in diameter into 20 channels. The width of each channel is irregular, ranging from 0.1 to 0.5 mm. In the presence of heavy rain, the JW disdrometer underestimates the small drops because of the inherent dead time of the sensor due to ringing of the mechanical system after the impact of a large drop. The number of small drops is also underestimated because of acoustic noise, strong winds, or electrical interference (D. Högl 2006, personal communication). Among these factors, strong winds play an important role in tropical cyclones. The RSD measurements taken during Hurricane Rita (2005) in Lafayette and Hurricane Ernesto (2006) in Wallops Island showed severe underestimation of small and midsize drops where the peak concentration was around 1.87 mm in diameter at 40 dBZ. The maximum daily wind speed measured by Automated Weather Observing Systems was 40 and 49 kt in Rita and Ernesto, respectively. The midsize drops contribute significantly to the rain rate and reflectivity at moderate-to-heavy rain, and therefore these events were excluded from this study.

The JW disdrometer cannot resolve the size of raindrops larger than 5 mm in diameter. This is relatively less important in oceanic rainfall than in continental rainfall since the maximum drop diameter rarely exceeds 5 mm in oceanic systems including tropical cyclones. The disdrometer also assumes that the raindrops fall at their terminal fall speed. In the presence of updrafts and downdrafts, the raindrop size can be under- or overestimated (Salles and Creutin 2003). The disdrometer occasionally reports spurious large drops during light-to-moderate rain. These drops can be easily identified through examining the time series of the RSD.

3. Raindrop size distribution

Among various RSD models, the three-parameter gamma model has been widely used in the atmospheric sciences community and represents the observed raindrop spectra reasonably well (Tokay and Short 1996). The gamma size distribution is expressed as

$$N(D) = N_0 D^m \exp(-\Lambda D), \tag{1}$$

where N_0, Λ, and m are the intercept, slope, and shape parameters, respectively.

The gamma model is also employed in studies that deal with the retrieval of the RSD from dual-frequency or dual-polarized radar measurements for the purposes of improving global precipitation estimates (Rincon and Lang 2002; Brandes et al. 2003). However, these studies usually lack a third measurement for the re-

trieval algorithm. They either assume a constant shape parameter or seek a relation between the parameters of the gamma model. Zhang et al. (2001), for example, offered a relation between slope and shape parameters of the gamma function. Cloud modeling studies, on the other hand, often use the exponential size distribution where the shape parameter of the gamma distribution is set to zero (Tao and Simpson 1993).

Since radar measurements are an integral product of the RSD, there has been an interest in expressing the gamma model distribution with observed variables. Bringi et al. (2003), for instance, substituted the slope parameter with the mean mass diameter D_{mass}, which is the ratio of the fourth to the third moment of the size distribution:

$$\Lambda = \frac{4 + m}{D_{\text{mass}}}. \tag{2}$$

They also substituted the intercept parameter with an expression that includes the liquid water content W and mean mass diameter. This alternative normalized intercept parameter N_w is expressed as

$$N_w = \frac{256W}{\pi\rho_w D_{\text{mass}}^4}, \tag{3}$$

where ρ_w is the density of water. In this study, we adopted a similar representation of the gamma model distribution where the intercept parameter is normalized based on number concentration N_T and mean mass diameter:

$$N_0 = N_T \frac{(4 + m)^{m+1}}{(D_{\text{mass}})^{m+1}\Gamma(m + 1)}. \tag{4}$$

The normalized gamma model distribution is then expressed substituting Eqs. (2) and (4) into Eq. (1):

$$N(D) = N_T^* f(m)\left(\frac{D}{D_{\text{mass}}}\right)^m \exp\left[-(4 + m)\frac{D}{D_{\text{mass}}}\right], \tag{5}$$

where N_T^* is the normalized intercept parameter and is the ratio of the number concentration to the mean mass diameter, and

$$f(m) = \frac{(4 + m)^{m+1}}{\Gamma(m + 1)}. \tag{6}$$

The number concentration is proportional to the zero moment of the drop diameter and is typically underestimated in disdrometer measurements because of the instrument shortcomings listed in the previous section. The liquid water content is related to the third moment of the size distribution and is mainly contributed by the midsize drops that are well represented in disdrometer measurements (Tokay et al. 2001, 2002). Therefore, the normalization of the RSD by the liquid water content may be more attractive than the normalization by the number concentration at first glance, but the integral parameters that are proportional to the low moments of the spectra will have high errors when they are calculated from the gamma model distribution. In that regard, Smith (2003) recommends the central moments (second, third, and fourth) for a general representation of the gamma model distribution.

While the mean mass diameter and number concentration can be calculated from disdrometer measurements, a third integral parameter is required to determine the shape parameter. For the purpose of this study, we selected the rain rate such that the shape parameter was calculated minimizing the root-mean-square difference between the disdrometer-calculated and gamma model [Eq. (5)]–based rain rate.

To determine the characteristics of the RSD in tropical cyclones, we averaged the 1-min disdrometer observations at 2-dB intervals centered at 40 dBZ. Averaging the RSD based on reflectivity is similar to the sequential intensity filtering technique described by Lee and Zawadzki (2005). In their study, the averaging by reflectivity or rain-rate interval was performed to reduce the noise around the Z–R relation. The averaging by reflectivity or rain-rate interval rather than averaging by a selected time window (e.g., 5 min) can be problematic if there are characteristic differences of the RSD within the system. Tokay and Short (1996), for instance, showed the characteristic differences of RSD in convective and stratiform regions of tropical storms at the same rain rate. This is why we considered 40 dBZ, which represents the convective region with a sufficient sample size. We considered the sample size of five or more 1-min spectra as sufficient to extract the physical characteristics of the RSD. The sample size is typically less than this threshold at reflectivity intervals above 40 dBZ.

4. Synoptic settings

Brief synoptic settings were documented for seven storms during the 2004–06 Atlantic hurricane seasons through the tropical cyclone reports presented on the National Hurricane Center Tropical Prediction Center Web page. A summary of synoptic settings including the maximum wind speed and minimum surface pressure at the time where rainfall was observed at the observation sites is presented in Table 1. Table 1 also includes the rainfall totals from collocated disdrometer and tipping-bucket gauges, rainy minutes from dis-

TABLE 1. Synoptic settings of the tropical cyclones including maximum wind speed and the lowest surface pressure at the time of observation. The disdrometer and gauge rainfall, disdrometer rainy minutes, and maximum sustained wind speed near the observation site are also given.

Tropical cyclone	Observation site	Max wind speed (kt) and the lowest surface pressure (mb) of the tropical cyclone	Disdrometer and gauge rainfall (mm) and disdrometer rainy minutes	Max wind speed (kt) and the time and date of occurrence
Alex (2004)	Wallops Island, VA	85, 972	42, 42, 338	14 at 1338 UTC 3 Aug
Charley (2004)	Wallops Island, VA	60, 1000	70, 75, 713	20 at 1554 UTC 14 Aug
Gaston (2004)	Wallops Island, VA	35, 1000	15, 18, 279	21 at 0718 UTC 30 Aug
Matthew (2004)	Lafayette, LA	40, 1000	136, 155, 1379	22 at 1924 UTC 8 Oct
Cindy (2005)	Wallops Island, VA	20, 1010	17, 18, 209	21 at 0016 UTC 8 Jul
Tammy (2005)	Wallops Island, VA	—	57, 65, 1091	25 at 1007 UTC 8 Oct
Alberto (2006)	Orlando, FL	60, 997	24, 28, 511	22 at 1653 UTC 12 Jun
Alberto (2006)	Wallops Island, VA	35, 1002	53, 55, 920	15 at 1223 UTC 14 Jun

drometer observations, and maximum wind speed and its time of occurrence near the observation site. For the accuracy of the disdrometer measurements, it is ideal that the rainbands of the storm pass the observation site under weak wind conditions. This is, of course, not feasible for every tropical cyclone. As previously mentioned, two hurricanes were disregarded because of strong winds that had a pronounced effect on the RSD measurements. In addition, the forecast of the landfall of Hurricane Isabel (2003) was just south of Wallops Island and all the instruments were dismounted as a precaution. The remnants of Hurricane Gordon (2000), Tropical Storm Helene (2000), and Tropical Storm Allison (2001) had light-to-moderate rainfall at Wallops Island where the number of the raindrop spectra at 40 dBZ was insufficient to determine the characteristics of the RSD and therefore these cases were not included in this study.

Hurricane Alex (2004) was the first storm that is examined here and was unique for two reasons. First, it never made landfall but resulted in substantial rainfall in the Carolinas and Virginia. Second, it was the second major hurricane above 38°N after Hurricane Ellen (1953). Alex became a category 1 hurricane based on the Saffir–Simpson scale at 0600 UTC on August 3 (Fig. 1a). During the period where rainfall was observed at Wallops Island, the maximum sustained winds reached 85 kt and minimum surface pressure fell to 972 mb 6 h later (Table 1). After degrading back to a category 1 hurricane, Alex reintensified and became a category 3 hurricane at 0000 UTC 5 August as it moved east-northeast.

Hurricane Charley (2004) was a powerful and long-lasting storm. At the time, it was listed as the strongest hurricane (category 4) that hit the United States since Hurricane Andrew (1992). It crossed Florida and North Carolina where it finally degraded to a tropical storm (Fig. 1b). During its movement over North Carolina, Charley interacted with a frontal zone and was eventually embedded in the frontal zone when it began moving back into the Atlantic Ocean in the vicinity of Virginia Beach, Virginia.

Hurricane Gaston (2004) reached its hurricane strength just before it made landfall on the South Carolina coast at 1200 UTC 29 August, but degraded to a tropical storm and then tropical depression within 12 h (Fig. 1c). Despite its rapid weakening, Gaston crossed over North Carolina and Virginia and caused flooding. Eight casualties were reported in or around Richmond, Virginia, where flooding was heaviest. Gaston reached tropical storm strength as it crossed the Chesapeake Bay at 0000 UTC 31 August. It also crossed just south of Wallops Island before it moved over the Atlantic Ocean.

Unlike the previous three storms, Tropical Storm Matthew (2004) formed as a tropical depression in the Gulf of Mexico and reached its maximum strength of 40 kt at 1800 UTC 9 October (Fig. 1d). Matthew degraded to a tropical depression right after it made landfall approximately 173 km west of New Orleans, Louisiana.

Hurricane Cindy (2005) made its first U.S. landfall approximately 50 km southwest of New Orleans, Louisiana, at 0300 UTC 6 June, just 54 days before catastrophic Hurricane Katrina (Fig. 1e). While Cindy left 75 mm of rain in New Orleans, no rainfall was observed at the disdrometer site in Lafayette, Louisiana. During its northeasterly path following its second landfall in southwestern Mississippi, Cindy degraded to a tropical storm, and then to a tropical depression in southwest Alabama. Cindy merged with a stationary front and became an extratropical low in northern Georgia. The system continued its northeastward movement along the eastern slopes of the Appalachian Mountains of western North Carolina and western Virginia, and

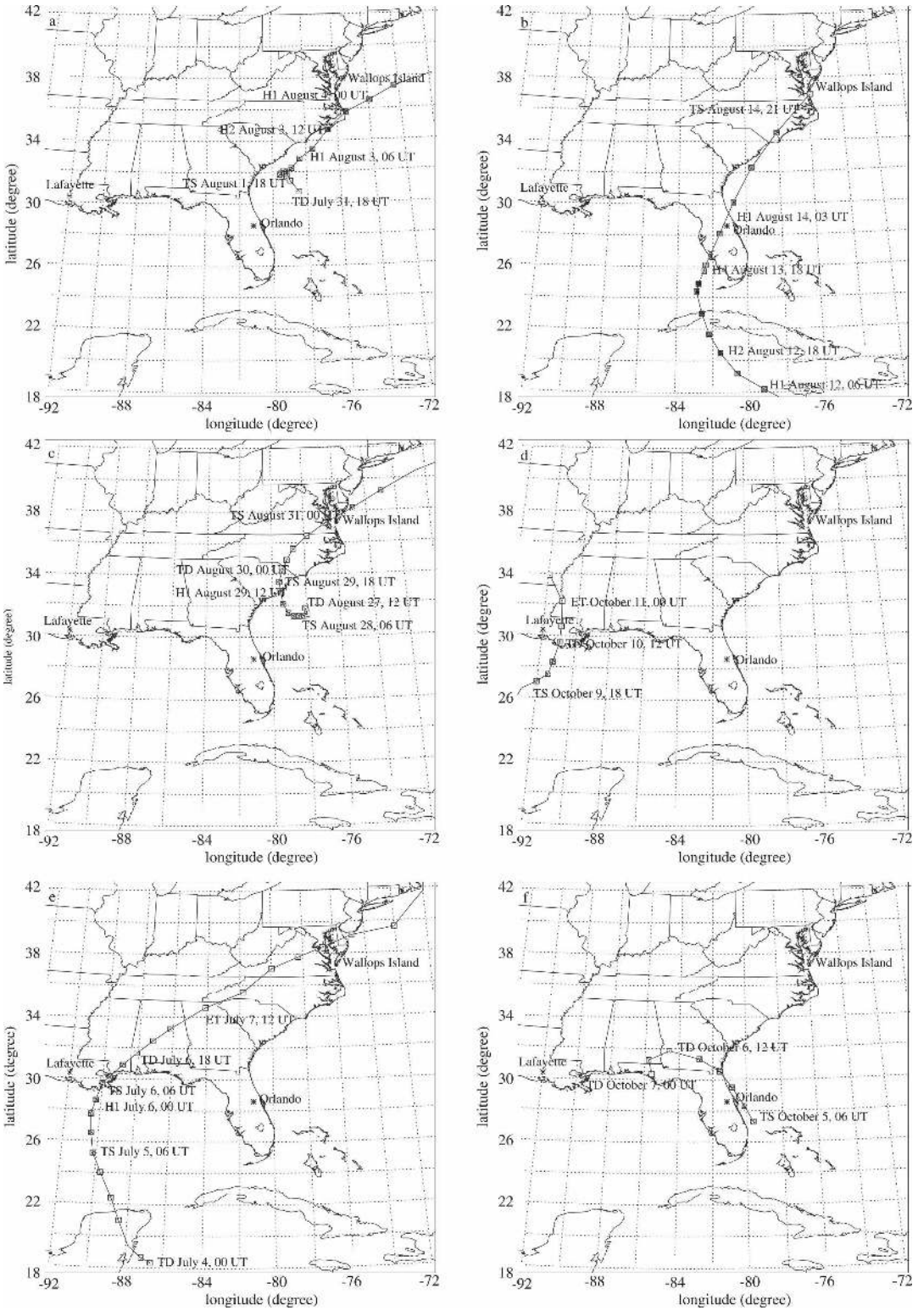

FIG. 1. Tropical cyclone track maps for (a) Hurricane Alex, (b) Hurricane Charley, (c) Hurricane Gaston, (d) Tropical Storm Matthew, (e) Hurricane Cindy, (f) Tropical Storm Tammy, and (g) Tropical Storm Alberto. The maps were redrawn following the National Hurricane Center Tropical Prediction Center Web page. The Saffir–Simpson intensity scale of tropical cyclones is given to the right of (g) (facing page).

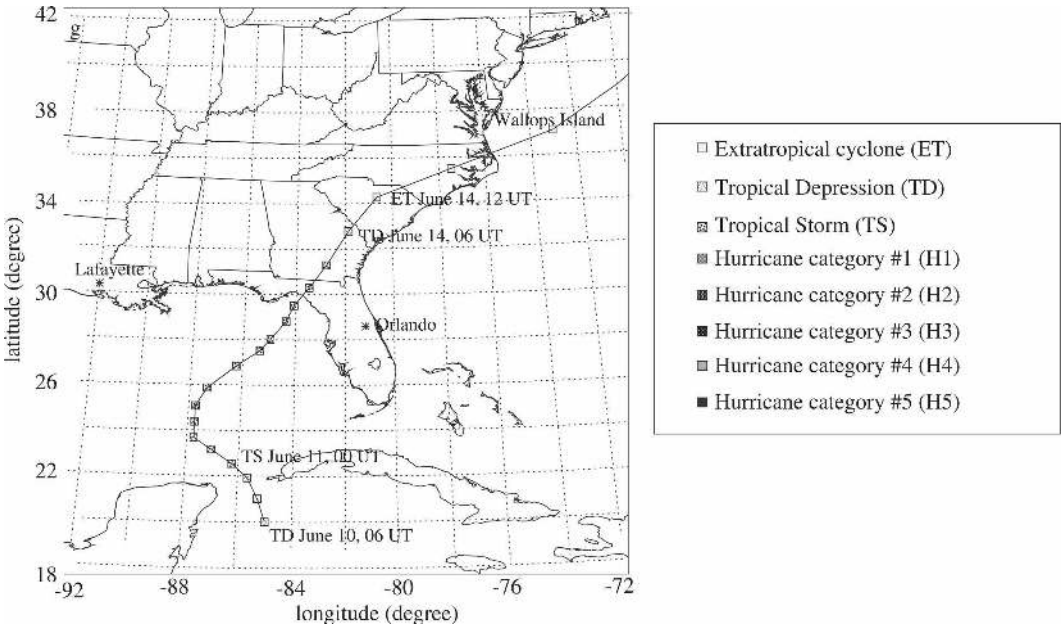

FIG. 1. (*Continued*)

crossed Maryland and Delaware before it emerged off the mid-Atlantic coast of the United States. As an extratropical low, Cindy produced heavy rainfall and caused local flooding in many areas of eastern Tennessee, western North Carolina, and Virginia.

Tropical Storm Tammy (2005) formed as a tropical storm about 206 km southeast of Orlando, Florida, at 0600 UTC 5 October (Fig. 1f). Under the influence of a southeasterly steering flow to the east of the cyclone, Tammy moved northwestward, paralleling the Florida east coast and making landfall on the northeast Florida coast at around 2300 UTC. Tammy degraded to a tropical depression in Georgia at 1200 UTC 6 October. Under the influence of a southerly flow in front of a north–south-oriented cold front, the moisture from Tammy was carried northeastward, bringing substantial rainfall from Georgia to New Hampshire. Since Tammy was never in the vicinity of the observation site, its synoptic settings were not included in Table 1.

Following its tropical depression stage east of the Yucatán peninsula, Tropical Storm Alberto (2006) became a tropical storm at 0000 UTC 11 June and remained at this stage for three days after it made landfall in northern Florida (Fig. 1g). Alberto began to lose tropical characteristics over South Carolina, became extratropical at 1200 UTC 14 June, and then moved back over the Atlantic Ocean, where it became a powerful extratropical storm just south of Nova Scotia, Canada. Alberto was unique for this study since its rainfall was observed at two different locations.

5. Time series of raindrop size distribution

The time series of the RSD during the passage of Hurricane Alex revealed three different segments that were separated by rain intermittence of half an hour to an hour except for brief spells of light rain (Fig. 2a). The first segment exhibited the event's highest reflectivity, 49 dBZ, and maximum rain intensity, 55 mm h^{-1}, occurring just 2 min apart at around 1030 UTC. The relatively high concentrations of midsize drops with the presence of large drops were responsible for the heavy rain and high reflectivity. The small drops were not adequately measured in the spectra resulting in relatively low drop concentrations during heavy rain. This could be due to the disdrometer's dead time. For a 1-h period near the end of the first segment starting at 1200 UTC, large concentrations of small drops were present in the narrow raindrop spectra where the maximum drop diameter was 2.4 mm. Interestingly, the event's highest concentration, 1301 drops m^{-3}, was observed at this period where rain rate was 15 mm h^{-1} and the reflectivity was 37 dBZ. The middle portion of the second regime segment exhibited a high concentration of midsize drops while an appreciable number of larger drops were also present. The reflectivities were above 39 dBZ for nearly a half hour period starting at 1516 UTC. The last segment of the storm had low concentrations of small and midsize drops, with the maximum drop diameter not exceeding 2.6 mm except for a peculiar spectrum at 1832 UTC where two large drops

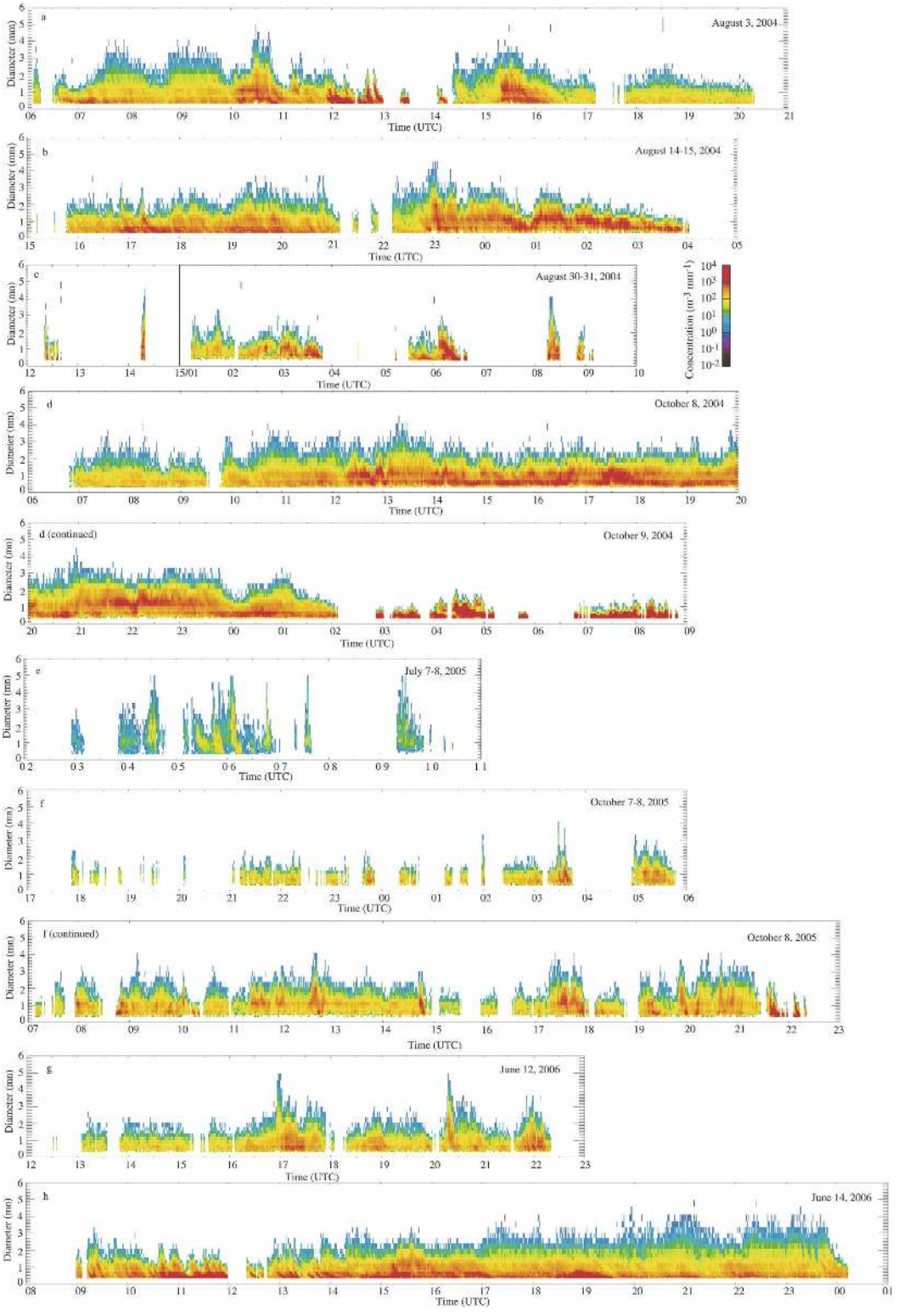

FIG. 2. Time series of raindrop size distribution for (a) Hurricane Alex, (b) Hurricane Charley, (c) Hurricane Gaston, (d) Tropical Storm Matthew, (e) Hurricane Cindy, (f) Tropical Storm Tammy, (g) Tropical Storm Alberto in Orlando, FL, and (h) Tropical Storm Alberto in Wallops Island, VA. The scale for the drop concentration is given next to (c).

were observed. These spurious large drops resulted in the event's maximum mean mass diameter, and the water content had doubled in value with respect to its neighboring minutes. This illustrates the significance of measurement errors in calculated rain parameters.

The time series of the RSD during Hurricane Charley's passage showed two different segments that were separated by rain intermittence of 1 h except for brief spells of light rain (Fig. 2b). The large number of small drops and the lack of large drops were observed during the first segment of the storm. The second segment of the storm, on the other hand, had relatively higher concentrations of midsize drops, and large drops were present particularly at around 2300 UTC. The storm's higher reflectivities and rain rates were observed within the 2-h period following 2300 UTC as well.

Rainfall was quite sporadic during Tropical Storm Gaston's passage over Wallops Island. Following two brief periods of rain around 1230 and 1420 UTC 30 August, a period of no rain was observed over 10 h (Fig. 2c). High concentrations of small and midsize drops were observed during the second period of brief showers where the reflectivities were high and rain was intense. Most of the rainfall fell during the 3-h period starting after 0100 UTC 31 August. High concentrations of midsize drops were observed toward the end of this rainy period and during the next segment of the rain that lasted over an hour at around 0600 UTC. Two faulty large drops were noticed at 0212 UTC. As at the beginning, the passage of Gaston ended with two brief showers where high concentrations of small and midsize drops were present.

The time series of RSD during Tropical Storm Matthew's passage exhibited three different segments of the storm (Fig. 2d). The first segment lasted over 2 h 30 min and a few large drops were occasionally observed in the presence of relatively low concentrations of small and midsize drops. The second and the most impressive segment of the storm had a 16-h duration continuous rainfall where high concentrations of small drops were persistent for 7 h starting at 1400 UTC. The presence of high concentrations of midsize drops was observed for nearly an hour around 2200 UTC and large drops (>4 mm in diameter) were present right after 1300 UTC and right before 2100 UTC. These high concentrations of midsize drops and the presence of large drops resulted in higher reflectivities that were included in the composite spectra at 40 dBZ. The third segment of the storm had large concentrations of small drops but the size distributions were narrow where the maximum drop diameter was less than 2 mm in diameter. Although both first and third segments of the storm exhibited mostly light rain (<1 mm h^{-1}), the size distributions were very different from each other.

The time series of the RSD during the passage of Hurricane Cindy passage was substantially different than previous storms. The depletion of small drops was well marked (Fig. 2e). Unlike the previous four storms, there was no segment in the time series where high concentrations of small and midsize drops were observed. Recall that Cindy was an extratropical cyclone at the time of observations, hinting at distinctly different characteristics of RSD in a tropical cyclone before and after the extratropical stage.

Tropical Storm Tammy was the longest rain event at Wallops Island, but rain intermittence was frequently observed until 0900 UTC 8 October. The high concentrations of midsize drops and the presence of large drops (>4 mm in diameter) were observed just before 1300, 1800, and 2100 UTC 8 October (Fig. 2f). The concentrations of small drops were high just before 1300 and 1800 UTC and around 2000 and 2200 UTC 8 October. Despite the fact that the Tammy was no closer than about 1000 km to the disdrometer site, the RSD features including high number density of small and midsize drops and noticeable large drops matched well with previous storms except Cindy.

During Tropical Storm Alberto's passage in Orlando, periods of high concentrations of small and midsize drops were observed right after 1700 UTC and around 2200 UTC (Fig. 2g), while large drops (>4 mm in diameter) were present in very brief periods at 1700 UTC and just before 2030 UTC. These characteristics were somewhat different than the RSD characteristics of the first four storms examined above, mainly due to the relatively brief periods of high concentrations of midsize drops. At Wallops Island, high concentrations of small drops were observed throughout the storm, but high concentrations of midsize drops were limited to within a 1-h period following 1500 UTC (Fig. 2h). The large drops had relatively high concentrations after 1700 UTC resulting in high reflectivity periods. These characteristics may resemble the passage of an extratropical storm, but substantial differences between the time series of Hurricane Cindy and Tropical Storm Alberto were evident.

6. Composite raindrop spectra

Since Hurricane Alex never made landfall, did not interact with a frontal system, and left substantial rainfall at relatively weak wind speeds, the composite raindrop spectra were considered as a reference tropical cyclone in this study. The composite spectra had a maximum drop diameter of 4.07 mm, and the drop con-

centration increased with decreasing drop diameter until diameter was 1.10 mm (Fig. 3a). The maximum concentration occurred at a diameter of 0.54 mm followed by a local minimum at 0.76 mm in diameter. The local minimum and the decrease in concentration and size following maximum concentration were attributed to the quantization and measurement errors. Except for number concentration, the integral rain parameters were not affected by the lack of small drops. The midsize drops contributed more than 90% of the water content and rain rate. They also contributed more than half of the number concentration (Table 2). The mean mass diameter was 1.69 mm.

The characteristics of the RSD in Hurricanes Charley and Alex were in good agreement, particularly in midsize drops (Fig. 3a). The composite spectra in Charley had fewer small and large drops, resulting in a relatively smaller number concentration than the spectra in Alex (Table 2). The water content and rain rate were slightly less in Charley since both parameters are mainly sensitive to the midsize drops. The mean mass diameters were about the same in both storms.

Despite a much smaller sample in composite spectra, the characteristics of RSD in Hurricane Gaston were in good agreement with the previous two storms (Fig. 3a). As in Hurricane Charley, the composite spectra had fewer large drops in Gaston than in Alex. The number of midsize drops was relatively higher in the Gaston raindrop spectra than the previous storms resulting in higher number concentrations (Table 2). The water content and rain rate was therefore also relatively higher in Hurricane Gaston. The mean mass diameter was slightly less in Gaston than the previous two storms.

The composite spectra of Tropical Storm Matthew had good agreement with the spectra of the previous three storms (Fig. 3a). The concentrations of small drops (<0.76 mm in diameter) were relatively less, while the concentrations of large drops were somewhere in between the spectra of Alex and Charley. The number concentration, water content, and rain rate were all within the range of previous storms (Table 2). The mass median diameter was about the same as the first two storms. Considering that Matthew's observations were taken at a different site with a different disdrometer, this boosted our confidence of observing the expected range of RSD parameters in tropical cyclones.

The composite spectra of Hurricane Cindy differed substantially from the spectra of previous storms. The spectra had considerably fewer small drops and more large drops where the crossover was at 2.7 mm in diameter (Fig. 3b). The number concentration, water content, and rain rate calculated from the composite spectra of Cindy were lower than the previous storms due to fewer small and midsize drops in Cindy's composite spectra (Table 2). These integral parameters also had a higher contribution from larger drops than the previous storms. The mean mass and maximum drop

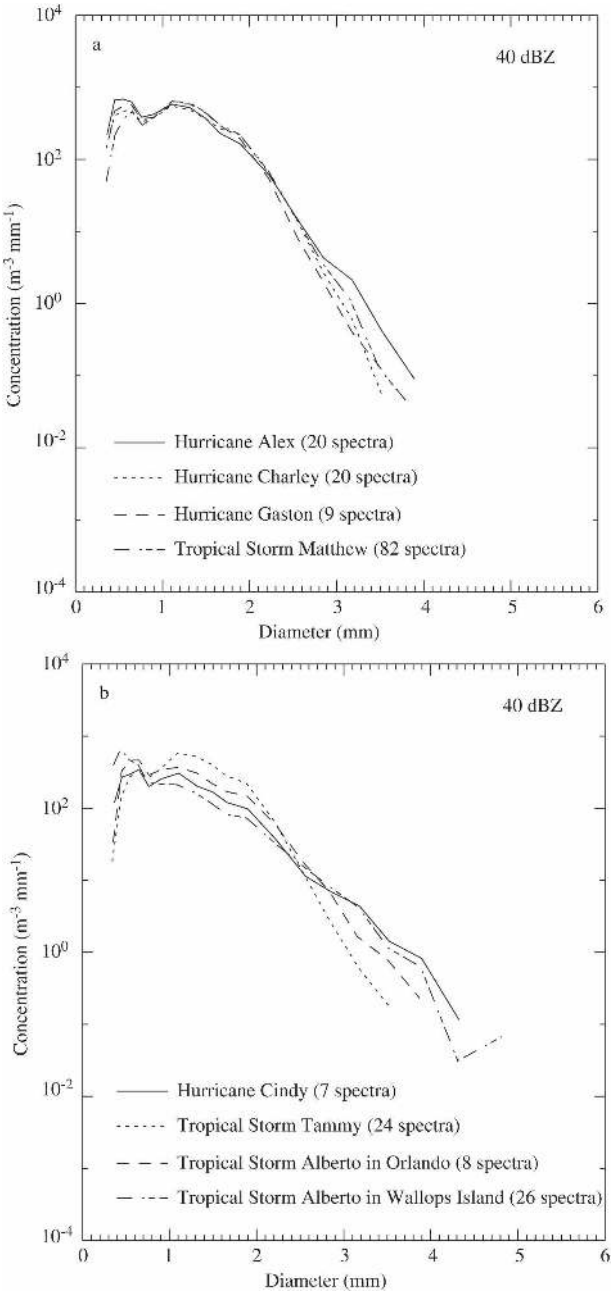

FIG. 3. The composite raindrop spectra for (a) Hurricane Alex, Hurricane Charley, Hurricane Gaston, and Tropical Storm Matthew; and (b) Hurricane Cindy, Tropical Storm Tammy, and Tropical Storm Alberto in Orlando, FL, and in Wallops Island, VA. The number of 1-min observations is also given for each case.

TABLE 2. Integral rain parameters in tropical cyclones that were derived from composite raindrop spectra at 40 dB*Z*.

Tropical cyclone	Total concentration (No. of drops m^{-3})	Liquid water content (g m^{-3})	Rain rate (mm h^{-1})	Mean mass diameter (mm)	Max drop diameter (mm)
Alex (2004)	778	0.878	18.1	1.69	4.11
Charley (2004)	663	0.863	17.9	1.70	3.71
Gaston (2004)	793	0.974	19.8	1.64	3.71
Matthew (2004)	671	0.925	19.1	1.68	4.07
Cindy (2005)	369	0.495	10.9	1.92	4.57
Tammy (2005)	597	0.874	18.1	1.69	3.71
Alberto in Orlando (2006)	511	0.667	14.3	1.80	4.06
Alberto in Wallops Island (2006)	403	0.420	9.4	1.98	5.00

diameters were larger in Cindy's spectra than the previous storms. These systematic differences in Hurricane Cindy's spectra were attributed to the extratropical nature of the storm, where rainfall at Wallops Island occurred well after the tropical system merged with a stationary front.

The composite spectra of Tropical Storm Tammy agreed well the first four storms in all size regimes except at small drop sizes less than 0.76 mm in diameter (Fig. 3b). The water content and rain rate were within the bounds of the first four storms, while the number concentration was relatively low, but still well above Hurricane Cindy's spectra (Table 2). The presence of fewer small drops was the main reason for the relatively lower number concentration. The mean mass and maximum drop diameters were also within the range of first four storms.

The composite spectra of Tropical Storm Alberto in Orlando exhibited fewer midsize drops (1–2 mm in diameter) than the spectra of other storms except Cindy, while the agreement of the small and large drops was reasonable (Fig. 3b). The presence of fewer midsize drops resulted in a smaller number concentration, water content, and rain rate in Alberto than the other storms except Cindy (Table 2). The mean mass diameter, on the other hand, was relatively higher as expected.

In many aspects, the composite spectra of Alberto at Wallops Island resembled the composite spectra of Cindy. In comparison to Cindy, the concentration of the midsize drops was lower in Alberto at diameters less than 2.38 mm (Fig. 3b). At sizes less than 0.76 mm, the spectra of Alberto had higher concentrations than Cindy, while both Cindy and Alberto had similar concentrations of large drops. The water content and rain rate was the lowest because of fewer midsize drops, while the number concentration was relatively higher than Cindy (Table 2). The mean mass and maximum drop diameters in Alberto were also the highest among all storms examined above.

7. Raindrop size distribution measurements in the central tropical Pacific

Measurements of RSD have been collected by a JW disdrometer at Roi-Namur Island (9.39°N, 167.47°E) of the Republic of Marshall Islands. Roi-Namur is located on the northern edge of the Kwajalein Atoll, which serves as the TRMM oceanic ground validation site (Wolff et al. 2005). It receives precipitation from organized and isolated convective cells when the Pacific intertropical convergence zone is in its northerly position (Schumacher and Houze 2003).

During May–December 2003, the JW disdrometer recorded 1375 mm of rainfall in 320 rainy hours. Two cases were selected for this study: one represented organized convective cells, and the other represented isolated convective cells. The first case occurred on 27–28 July, where the disdrometer recorded 80 mm of rainfall in 380 rainy minutes. For the first 2 h of the storm, the concentrations of small and midsize drops (1–2 mm in diameter) were high and large drops were absent (Fig. 4a). The large drops were present during the third hour of the storm and another hour centering at 1300 UTC. The concentrations of small and midsize drops were quite different between the two periods where large drops were observed. The high concentrations of small and midsize drops during the third hour of the storm indicates convective rain, while their relatively low concentrations later in the storm resemble stratiform rain. Interestingly, the time series of the RSD had similar structure with another storm that was analyzed in depth in Tokay and Short (1996) and Tokay et al. (1999).

The second case occurred on 19–20 December where the disdrometer recorded 92 mm of rainfall in 545 rainy minutes. Unlike the previous case, frequent rain intermittence was evident but it was less than an hour on each occasion. High concentrations of small and midsize drops were observed throughout the storm, while large drops were mostly present during the first 8 h of the storm (Fig. 4b).

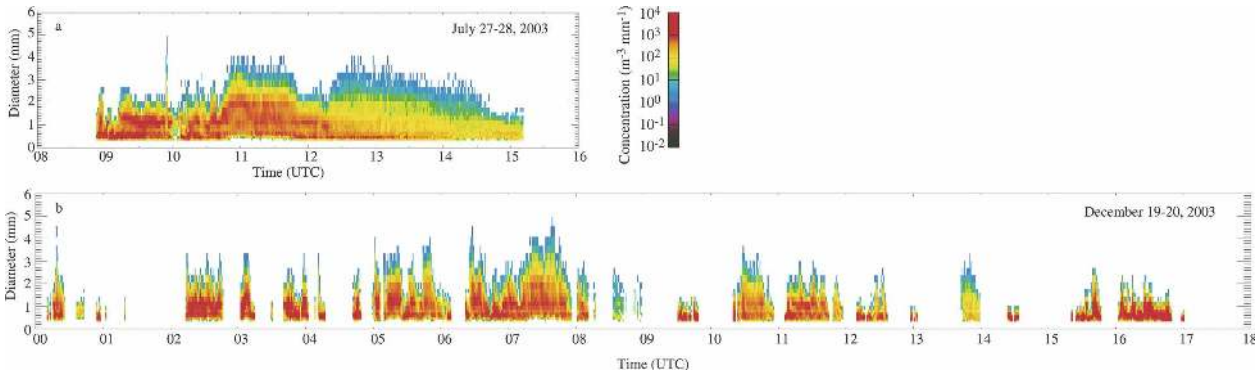

FIG. 4. Time series of raindrop size distribution for (a) 27–28 Jul 2003 and (b) 19–20 Dec 2003 rain events that were observed on Roi-Namur Island. The scale for the drop concentration is given next to the first case graph.

As in tropical cyclone cases, the composite raindrop spectra were constructed at 40 dBZ and the agreement between the two cases was excellent in a midsize drop range of 1.8 to 2.3 mm in diameter. At sizes less than 1.8 mm in diameter, the second case had more drops, while the reverse was true at sizes above 2.3 mm in diameter (Fig. 5). Nevertheless, the integral rain parameters that were derived from composite spectra had very good agreement including identical mean mass diameters between the two cases (Table 3). To compare the RSD from these two cases with the RSD of the tropical cyclones, we constructed composite spectra combining the observations of Alex, Charley, Gaston, and Tammy. We selected these storms since they were observed with the same disdrometer unit. Considering that each unit has its own calibration table and the size ranges vary slightly between units, this was an optimum choice. The composite spectra of tropical cyclones had fewer drops than spectra at Roi-Namur up to 1.8 mm in diameter, while the reverse was true at sizes above 2.3 mm in diameter (Fig. 5). The mean mass diameter was larger and the integral rain parameters of number concentration, liquid water content, and rain rate were smaller in tropical cyclones than at Roi-Namur (Table 3).

8. Raindrop size distribution parameters

Aside from distinct differences in RSD characteristics between convective and stratiform rain at a given rain rate or reflectivity, the grouping of the individual observations by reflectivity range is an adequate alternative method to time averaging to overcome sampling fluctuations. For the analysis presented above, we examined the individual observations that were contributing to the composite spectra at 39–41 dBZ interval in an event. Nevertheless, the parameters of the RSD derived from very high and very low reflectivity regimes that represent convective and stratiform rain, respectively, will not satisfy the modeler or other interested scientists. Therefore, we derived the RSD parameters from composite spectra that represent the wide range of reflectivities even through there is an intrastorm variability of RSD. Prior to the derivation of the RSD parameters, we combined the observations from four tropical cyclones that had similar RSD characteristics

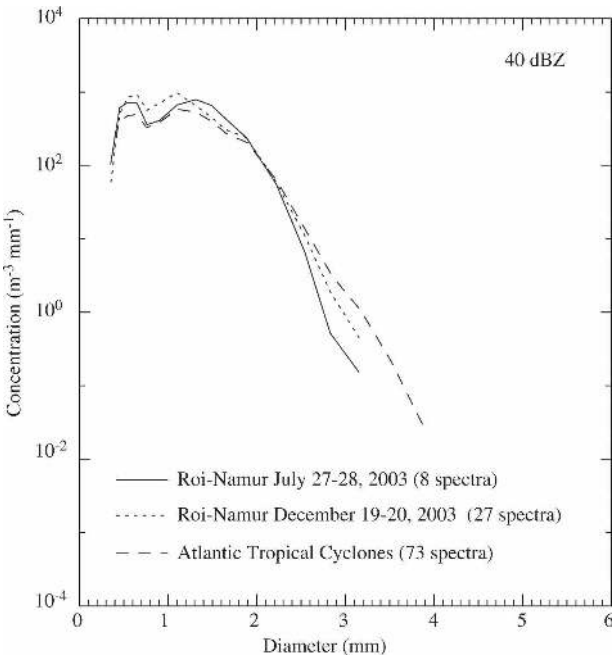

FIG. 5. The composite raindrop spectra for 27–28 Jul 2003 and 19–20 Dec 2003 rain events that were observed on Roi-Namur Island. The composite raindrop spectra of Atlantic tropical cyclones are included after the disdrometer observations from four tropical cyclones (Hurricane Alex, Hurricane Charley, Hurricane Gaston, and Tropical Storm Tammy) were merged. The number of 1-min observations is also given for each case.

TABLE 3. Integral rain parameters in two rain events in Roi-Namur and combined four events in tropical cyclones at 40 dBZ. The combined tropical cyclone events were Hurricane Alex, Hurricane Charley, Hurricane Gaston, and Tropical Storm Tammy.

Rain event	Total concentration (No. of drops m^{-3})	Liquid water content (g m^{-3})	Rain rate (mm h^{-1})	Mean mass diameter (mm)	Maximum drop diameter (mm)
27–28 Jul, Roi-Namur	903	1.086	21.8	1.59	3.32
19–20 Dec, Roi-Namur	982	1.038	20.6	1.59	3.32
Tropical cyclones	687	0.875	18.2	1.68	4.11

as we did in the previous section. The combined dataset had 2830 one-minute observations and allowed us to group the data based on 1-dB reflectivity intervals from 10 to 45 dBZ where each interval had at least 12 one-minute observations. We repeated the same exercise for the Roi-Namur dataset where each interval had at least 110 one-minute observations.

The mean mass diameter increased with reflectivity and there were no clear distinctions between the two datasets (Fig. 6a). The normalized intercept parameter also increased with reflectivity where number concentration was higher in Roi-Namur than in tropical cyclones (Fig. 6b). With respect to D_{mass}, N_T^* decreased from 0.6 to 0.8 mm, increased from 0.8 to 1.6 mm, and became steady between 1.6 and 2.0 mm (not shown). The decrease of N_T^* with increasing D_{mass} indicates the decrease of small drops, but this could be related to the instrument inability to measure the small drops accurately. The increase of N_T^* with increasing D_{mass} indicates the presence of more midsize and large drops, while the presence of more midsize and large drops is accompanied by a decrease of small drops in a regime where N_T^* is steady and D_{mass} is increasing. The disdrometer's dead time probably contributed to the decrease of small drops at high rain intensities. The alternative normalized intercept parameter demonstrated the same characteristics as the standard normalized intercept parameter with respect to reflectivity and mean mass diameter (not shown). The ratio of N_w to N_T^* was steady with an average value of 21. The shape parameter in tropical cyclone RSD decreased from 11 to 5 from 10 to 20 dBZ and remained between 5 and 6 for reflectivities above 20 dBZ (Fig. 6c). Like D_{mass}, the shape parameter did not show noticeable differences between the two datasets.

9. Conclusions

The characteristics of the RSD in tropical cyclones were studied through JW disdrometer observations in seven storms at three different sites during the 2004–06 Atlantic hurricane seasons. One of the storms, Tropical Storm Alberto, has been observed twice at two different sites. The time series of RSD showed high concentrations of small and midsize drops in the presence or absence of large drops in all tropical cyclones unless they were observed in extratropical stage. Even in the presence of large drops, the maximum drop diameter rarely exceeded 4 mm unless the storm was in the extratropical cyclone stage. This was consistent with the airborne RSD as presented in Willis (1984). As a result, high values of number concentration, liquid water content, and rain rate were evident at modest reflectivities. For example, at 40 dBZ, the number concentration was 700 ± 100 drops m^{-3}, while the liquid water content and rain rate were 0.90 ± 0.05 g m^{-3} and 18.5 ± 0.5 mm h^{-1}, respectively. The mean mass diameter, on the other hand, was 1.67 ± 0.3 mm. The storms that were observed in the extratropical cyclone stage resembled continental thunderstorms having higher mean mass and maximum drop diameter at 40 dBZ. The characteristics of the RSD in Atlantic tropical cyclones were similar to those observed in the central tropical Pacific Island of Roi-Namur. The number density at 40 dBZ was shifted toward smaller drops, resulting in higher number concentration, water content, and rain rate at the latter site. The mean mass and maximum drop diameters were also smaller in Roi-Namur than in Atlantic tropical storms.

At 40 dBZ, the NWS default and tropical Z–R results in 12 and 21 mm h^{-1} rainfall, respectively. This demonstrates that the default Z–R will underestimate the tropical cyclone rainfall while vice versa is true for the tropical Z–R. Baeck and Smith (1998), who examined radar and gauge rainfall during Hurricane Fran (1995), reported the underestimation of rainfall when default Z–R was employed.

One of the objectives of this study was to parameterize the RSD of tropical cyclones for modeling studies. In that regard, we presented the behavior of normalized gamma distribution parameters as a function of reflectivity. The mean mass diameter increased rapidly with reflectivity, while the normalized intercept parameter had an increasing trend with reflectivity. The alternative normalized intercept parameter that employs the liquid water content for normalization had a similar

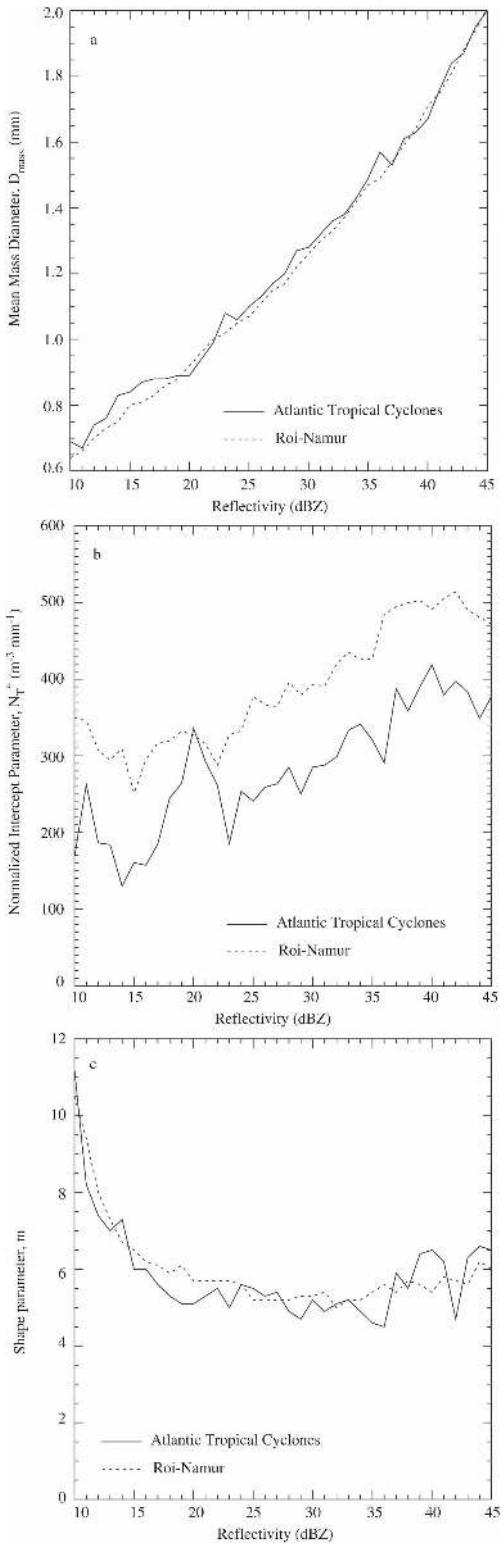

FIG. 6. The variability of normalized gamma size distribution parameters: (a) mean mass diameter, (b) normalized intercept parameter, and (c) shape parameter as a function of reflectivity. The parameters were derived from disdrometer observations that were collected in four Atlantic tropical cyclones (Hurricane Alex, Hurricane Charley, Hurricane Gaston, and Tropical Storm Tammy) and on Roi-Namur Island, and the parameters were grouped based on 1-dB*Z* reflectivity intervals.

trend as the standard normalized intercept parameter, which uses the number concentration. The shape parameter, which was determined through minimizing the root-mean-square difference between the disdrometer-calculated and gamma-model-derived rain rates, decreased from 10 to 20 dB*Z* and became steady at higher reflectivities.

As stated in the introduction, the extraction of the physical characteristics of the RSD from disdrometer measurements is not a straightforward task. The disdrometer measurements suffer from sampling and measurement errors. We grouped the disdrometer measurements by a reflectivity range that was adequate for the purpose of this study to overcome sampling errors. For the measurement errors, we excluded two tropical cyclones because of the presence of high wind speed and diagnosed false drops from the time series of the RSD. We also compared the disdrometer rain totals with collocated gauge rain totals. There are additional measurement errors that are specific to the JW disdrometer. In that regard, we tested the self-consistency of the characteristics of RSD by employing a second JW disdrometer near the primary disdrometer site for the same tropical cyclones (see the appendix). While the agreement in composite spectra between the sites was very good, the differences in the small and large ends of the size spectrum in one of the cases had a pronounced influence on number concentration and therefore modeled gamma distribution parameters. Another test of the repeatability of the characteristics of the RSD can be done through an analysis of other type disdrometer measurements in tropical cyclones. The two-dimensional video disdrometer is a good candidate and should be considered for future study.

Acknowledgments. We thank Richard Lawrence of NASA Goddard Space Flight Center and John Gerlach of NASA Wallops Flight Facility for their leadership in ground validation efforts of the TRMM program. The IDL programming that generated the color images of raindrop size distribution time series was done by Jordi Rosich of the Polytechnic University of Catalonia, Barcelona, Spain, and the preliminary analysis of the Roi-Namur disdrometer data were conducted by Rachel Albrecht of the University of São Paolo, São Paolo, Brazil. Discussions with Robert Meneghini of NASA

Goddard Space Flight Center and David Marks of George Mason University were very helpful. Support provided to the third author from the Louisiana Board of Regents Support Fund and the Louisiana LaSPCE space grant is acknowledged. We acknowledge four anonymous reviewers for their constructive comments. This study was supported by NASA's TRMM program through NAG5-13615, under Ramesh Kakar, Program Scientist.

APPENDIX

Self-Consistency of the Characteristics of Raindrop Size Distribution

The repeatability of the characteristics of RSD in tropical cyclones has been tested employing a second JW disdrometer in Wallops Island, where the distance between the units was 5.3 km. The primary site was called V50, while the second site was named Z65 after the building names where the disdrometers' indoor units were stored. Although the Z65 site was operational in all six tropical storms, we selected two storms in this study.

During the passage of Hurricane Charley, the disdrometer at the Z65 site recorded 73 mm of rainfall in 697 rainy minutes. The rain intensity was 6.3 mm h^{-1} on average, slightly higher than the intensity at the V50 site. The number of 1-min raindrop spectra at 40 dBZ in the Z65 site was almost double the number spectra in the V50 site. Nevertheless, the composite spectra at both sites had very good agreement in all size regimes (Fig. A1a). The composite spectra at the Z65 site had slightly more midsize drops between 1 and 2 mm in diameter, resulting in higher number concentration, water content, and rain rate at this site (Table A1). The mean mass diameter was slightly lower at the Z65 site spectra than in the V50 site spectra, while the maximum drop diameter was higher in the Z65 site spectra than in the V50 site spectra.

During Tropical Storm Alberto's passage, the disdrometer at Z65 recorded 57 mm of rainfall in 868 rainy minutes. The average rain intensity was 4.0 mm h^{-1}, higher than the intensity at the V50 site. The number of 1-min spectra at 40 dBZ in the Z65 site was more than double the number spectra in the V50 site. The composite spectra at both sites had very good agreement in the size range between 1.6 and 4.0 mm in diameter (Fig. A1b). At sizes less than 1.6 mm, the spectra at the Z65 site had considerably fewer drops resulting in a much smaller number concentration. The water content and rain rate were also smaller in the Z65 site spectra, but the difference was substantially less due to their higher sensitivity to the midsize and large drops (Table A1). The mean mass diameter at the Z65 site spectra was higher than the spectra at the V50 site owing to differences between the two spectra at both small and large

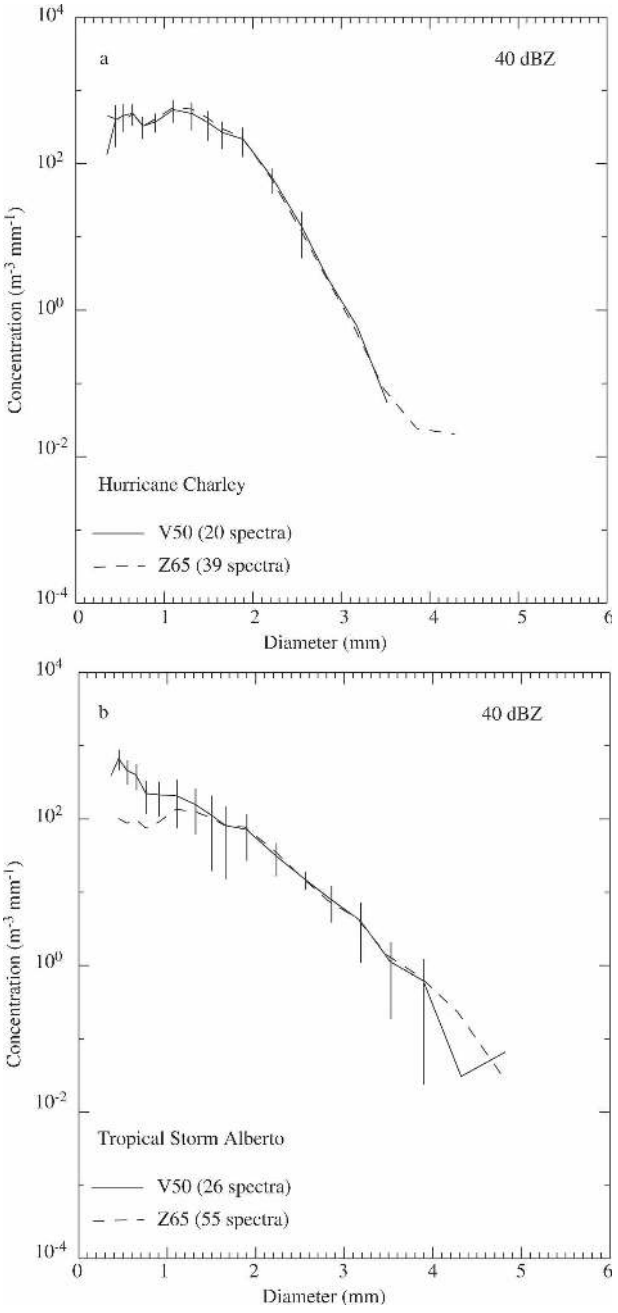

FIG. A1. The composite raindrop spectra for (a) Hurricane Charley and (b) Tropical Storm Alberto. The standard deviation of the measurements is provided for the primary site disdrometer. The composite is based on disdrometer observations at two different sites that were 5.3 km apart. The number of 1-min observations is also given for each case.

TABLE A1. Integral rain parameters in two Atlantic tropical cyclones that were observed by a second JW disdrometer located 5.3 km away from the primary disdrometer site at 40 dBZ.

Tropical cyclone	Total concentration (No. of drops m^{-3})	Liquid water content (g m^{-3})	Rain rate (mm h^{-1})	Mean mass diameter (mm)	Maximum drop diameter (mm)
Hurricane Charley (2004)	732	0.907	18.6	1.67	4.53
Tropical Storm Alberto (2006)	193	0.387	9.0	2.11	4.96

drop ends. The maximum drop diameter was about the same in both composite spectra.

The standard deviation of the number concentration was also shown for the primary site disdrometer in Fig. A1. The variability is relatively higher in both ends of the size spectrum. The natural variability was high between the individual spectra in the small drop end, while the absence of large drops in individual spectra was the leading reason of the high variability of the large drops in the composite spectra. The maximum drop diameter ranged between 2.56 and 3.52 mm in Hurricane Charley, while the range of maximum diameter was between 2.85 and 4.82 mm in Tropical Storm Alberto. The calculated standard deviations had therefore negative numbers at large drop diameters and are excluded in Fig. A1.

This study revealed that the characteristics of RSD in a tropical cyclone could be retrieved through JW disdrometer observations. The substantial discrepancy in number concentration in the second case, however, suggests that N_T^* may not be adequately retrieved. Indeed, this is a caveat of the parameterization of RSD based on disdrometer observations. The N_w parameter was not affected by the discrepancy in number concentration and had a good agreement in both cases.

REFERENCES

Baeck, M. L., and J. A. Smith, 1998: Rainfall estimation by the WSR-88D for heavy rainfall events. *Wea. Forecasting,* **13,** 416–436.

Brandes, E. A., G. Zhang, and J. Vivekanandan, 2003: An evaluation of a drop distribution-based polarimetric radar rainfall estimator. *J. Appl. Meteor.,* **42,** 652–660.

Bringi, V. N., G.-J. Huang, V. Chandrasekar, and E. Gorgucci, 2002: A methodology for estimating the parameters of a gamma raindrop size distribution model from polarimetric radar data: Application to a squall-line event from the TRMM/Brazil campaign. *J. Atmos. Oceanic Technol.,* **19,** 633–645.

——, V. Chandrasekar, J. Hubbert, E. Gorgucci, W. L. Randeu, and M. Schoenhuber, 2003: Raindrop size distribution in different climatic regimes from disdrometer and dual-polarized radar analysis. *J. Atmos. Sci.,* **60,** 354–365.

Fulton, R. A., J. P. Breidenbach, D.-J. Seo, D. A. Miller, and T. O'Bannon, 1998: The WSR-88D rainfall algorithm. *Wea. Forecasting,* **13,** 377–395.

Jorgensen, D. P., and P. T. Willis, 1982: A *Z-R* relationship for hurricanes. *J. Appl. Meteor.,* **21,** 356–366.

Joss, J., and A. Waldvogel, 1967: A spectrograph for the automatic analysis of raindrops (in German). *Pure Appl. Geophys.,* **68,** 240–246.

Lee, G. W., and I. Zawadzki, 2005: Variability of drop size distributions: Noise and noise filtering in disdrometric data. *J. Appl. Meteor.,* **44,** 634–652.

Maeso, J., V. N. Bringi, S. Cruz-Pol, and V. Chandrasekar, 2005: DSD characterization and computations of expected reflectivity using data from a two-dimensional video disdrometer deployed in a tropical environment. *Proc. Int. Geoscience and Remote Sensing Symp.,* Seoul, South Korea, IEEE, 5073–5076.

McFarquhar, G. M., and R. A. Black, 2004: Observations of particle size and phase in tropical cyclones: Implications for mesoscale modeling of microphysical processes. *J. Atmos. Sci.,* **61,** 422–439.

Merceret, F. J., 1974a: On the size distribution of raindrops in Hurricane Ginger. *Mon. Wea. Rev.,* **102,** 714–716.

——, 1974b: A note on the vertical distribution of raindrop size spectra in Tropical Storm Felice. *Meteor. Mag.,* **103,** 358–360.

Petersen, W. A., and Coauthors, 1999: Mesoscale and radar observations of the Fort Collins flash flood of 28 July 1997. *Bull. Amer. Meteor. Soc.,* **80,** 191–216.

Rincon, R. F., and R. H. Lang, 2002: Microwave link dual-wavelength measurements of path-average attenuation for the estimation of drop size distributions and rainfall. *IEEE Trans. Geosci. Remote Sens.,* **40,** 760–770.

Salles, C., and J.-D. Creutin, 2003: Instrumental uncertainties in *Z–R* relationships and raindrop fall velocities. *J. Appl. Meteor.,* **42,** 279–290.

Schumacher, C., and R. A. Houze Jr., 2003: The TRMM precipitation radar's view of shallow, isolated rain. *J. Appl. Meteor.,* **42,** 1519–1524.

Scott, W. D., 1974: In situ measurements of rainwater in Tropical Storm Felice and Hurricane Debby. *J. Meteor. Soc. Japan,* **52,** 440–447.

Smith, P. L., 2003: Raindrop size distributions: Exponential or gamma—Does the difference matter? *J. Appl. Meteor.,* **42,** 1031–1034.

Tao, W.-K., and J. Simpson, 1993: The Goddard cumulus ensemble model. Part I: Model description. *Terr. Atmos. Oceanic Sci.,* **4,** 19–54.

Tokay, A., and D. A. Short, 1996: Evidence from tropical raindrop spectra of the origin of rain from stratiform versus convective clouds. *J. Appl. Meteor.,* **35,** 355–371.

——, ——, C. R. Wiliams, W. L. Ecklund, and K. S. Gage, 1999: Tropical rainfall associated with convective and stratiform clouds: Intercomparison of disdrometer and profiler measurements. *J. Appl. Meteor.,* **38,** 302–320.

——, A. Kruger, and W. F. Krajewski, 2001: Comparison of drop

size distribution measurements by impact and optical disdrometers. *J. Appl. Meteor.,* **40,** 2083–2097.

——, ——, ——, P. A. Kucera, and A. J. Pereira Filho, 2002: Measurements of drop size distribution in the southwestern Amazon basin. *J. Geophys. Res.,* **107,** 8052, doi:10.1029/2001JD000355.

——, P. G. Bashor, and K. R. Wolff, 2005: Error characteristics of rainfall measurements by collocated Joss–Waldvogel disdrometers. *J. Atmos. Oceanic Technol.,* **22,** 513–527.

Ulbrich, C. W., and L. G. Lee, 2002: Rainfall characteristics associated with the remnants of Tropical Storm Helene in upstate South Carolina. *Wea. Forecasting,* **17,** 1257–1267.

Vieux, B. E., and P. B. Bedient, 1998: Estimation of rainfall for flood prediction from WSR-88D reflectivity: A case study, 17–18 October 1994. *Wea. Forecasting,* **13,** 407–415.

Williams, C. R., 2002: Simultaneous ambient air motion and raindrop size distributions retrieved from UHF vertical incident profiler observations. *Radio Sci.,* **37,** 1024, doi:10.1029/2000RS002603.

Willis, P. T., 1984: Functional fits to some observed drop size distributions and parameterization of rain. *J. Atmos. Sci.,* **41,** 1648–1661.

——, and P. Tattelman, 1989: Drop-size distributions associated with intense rainfall. *J. Appl. Meteor.,* **28,** 3–15.

Wilson, J. W., and D. M. Pollock, 1974: Rainfall measurements during Hurricane Agnes by three overlapping radars. *J. Appl. Meteor.,* **13,** 835–844.

Wolff, D. B., D. A. Marks, E. Amitai, D. S. Silberstein, B. L. Fisher, A. Tokay, J. Wang, and J. L. Pippitt, 2005: Ground validation for the Tropical Rainfall Measuring Mission (TRMM). *J. Atmos. Oceanic Technol.,* **22,** 365–380.

Zhang, G., J. Vivekanandan, and E. Brandes, 2001: A method for estimating rain rate and drop size distribution from polarimetric radar measurements. *IEEE Trans. Geosci. Remote Sens.,* **39,** 830–841.